Naval Research Laboratory
Washington, DC 20375-5000

NRL Memorandum Report 6633

Determination of the Heat Dissipated from a Specimen Undergoing Cyclic Plasticity by a Hybrid Numerical/Experimental Method

A. K. WONG AND G. C. KIRBY, III

Mechanics of Materials Branch
Materials Science and Technology Division

May 14, 1990

REPORT DOCUMENTATION PAGE

Form Approved
OMB No. 0704-0188

1. AGENCY USE ONLY (Leave blank)	2. REPORT DATE	3. REPORT TYPE AND DATES COVERED
	1990 May 14	

4. TITLE AND SUBTITLE

Determination of the Heat Dissipated from a Specimen Undergoing Cyclic Plasticity by a Hybrid Numerical/Experimental Method

5. FUNDING NUMBERS

PE - 61153N
PR - RR022-01-48
WU - 480-509

6. AUTHOR(S)

Wong, A. K. and Kirby, G. C., III

7. PERFORMING ORGANIZATION NAME(S) AND ADDRESS(ES)

Naval Research Laboratory
Washington, DC 20375-5000

8. PERFORMING ORGANIZATION REPORT NUMBER

NRL Memorandum Report 6633

9. SPONSORING/MONITORING AGENCY NAME(S) AND ADDRESS(ES)

Naval Sea Systems Command
Washington, DC 20362-5101

10. SPONSORING/MONITORING AGENCY REPORT NUMBER

11. SUPPLEMENTARY NOTES

12a. DISTRIBUTION/AVAILABILITY STATEMENT

Approved for public release; distribution unlimited.

12b. DISTRIBUTION CODE

13. ABSTRACT *(Maximum 200 words)*

A combined experimental/numerical approach is taken to decompose the hysteresis energy of a tensile specimen undergoing fully reversed plastic cycling into heat generation and internal energy in accordance with the first law of thermodynamics and the one dimensional diffusion equation with internal sources. Because of the difficulties in determining accurate boundary conditions and the sensitivity of the solution to the boundary conditions, the finite difference method was complemented with Lagrange multipliers. The sum of the square of the difference between the measured temperature and the predicted temperature at specific points along the specimen axis were minimized subject to the constraint of the finite difference template used. Results from preliminary tests indicate that when a critical energy density is reached failure occurs.

14. SUBJECT TERMS		15. NUMBER OF PAGES
Hysteresis energy	Lagrange multipliers	38
Fatigue	Optimization	16. PRICE CODE
One-dimensional diffusion equation		

17. SECURITY CLASSIFICATION OF REPORT	18. SECURITY CLASSIFICATION OF THIS PAGE	19. SECURITY CLASSIFICATION OF ABSTRACT	20. LIMITATION OF ABSTRACT
UNCLASSIFIED	UNCLASSIFIED	UNCLASSIFIED	SR

NSN 7540-01-280-5500

Standard Form 298 (Rev 2-89)
Prescribed by ANSI Std Z39-18
298-102

CONTENTS

DETERMINATION OF THE HEAT DISSIPATED FROM A SPECIMEN UNDERGOING CYCLIC PLASTICITY BY A HYBRID NUMERICAL/EXPERIMENTAL METHOD

INTRODUCTION

When a metallic specimen is deformed plastically, the bulk of the irreversible work is dissipated in the form of heat. It is generally accepted that the remaining part of the input energy is consumed by the change in the material's internal energy. Such internal energy changes can be attributed to phase changes, development of residual stresses, translation of dislocations; and the creation and/or enlargement of internal surfaces such as voids. Recent interests in deformation heating have primarily been motivated by metal forming processes where the substantial heat generation greatly influences the formability (e.g., [1]-[3]). However, the role of deformation heating in fatigue has also attracted some attention.

The earliest study on the energy dissipated by an oscillating solid was perhaps by Lord Kelvin [4]; who deduced that "dissipation of energy is an inevitable result of every change of volume." Other early studies include Hopkinson and Williams [5], and Haigh [6]. By using an extremely sensitive extensometer to measure the length of steel rods which had undergone complete and equal static load reversals, the authors in [5] found that even in the "elastic" regime, a minute permanent deformation was detectable. From this, they estimated the size of the stress-strain hysteresis area and thus the irreversible work. Using temperature measurements of similar specimens under fatigue load, they estimated that the heat dissipated is approximately 80% of hysteresis energy measured statically. The cause of this discrepancy was thought to be due to the fact that one test was done statically while the other was performed dynamically.

As mentioned earlier, we now know that the difference between the heat dissipated and the hysteresis energy is a real physical phenomenon which is associated with the change in energy state of the material. Consideration of the first law of thermodynamics quickly leads to the fact that if $\dot{W}$ is the irreversible work rate, and $\dot{Q}$ the heat dissipation rate, then for negligible kinetic effects, the rate at which energy is being accumulated within the material $\dot{U}$ is given simply by

$$\dot{U} = \dot{W} - \dot{Q}. \tag{1}$$

It is clear that a material cannot sustain an indefinite accumulation of energy. It has been proposed that $U(=\int \dot{U} \cdot dt)$ may be viewed as a "damage-energy," and that failure would occur when U reaches some critical value U_c (see [7], [8], and references within). The consequence of the existence of U_c can be enormous. If it can be established that U_c is indeed a material constant which is independent of loading and specimen geometry, then it could in principle be used for monitoring the residual strength of a component in service.

While this concept is elegantly simple, the determination of $\dot{U}$ (or U_c for that matter) is more complex. In a comprehensive survey on the determination of stored energy of cold worked metals, Bever et al. [9] identified two basic techniques (Single-step and Two-step methods) used to determine the energy stored in a cold worked metal. For the Single-step method, the work of deformation and heat dissipated (generally inferred from temperature measurements) are simultaneously monitored, and the stored energy is determined from the difference of these two quantities. Because such procedures involve the difference between two similarly sized quantities, it was shown that small relative errors

Manuscript approved February 27, 1990.

in each of the measurements can lead to large errors in the final result. For the Two-step methods, the stored energy is found by calorimetric means where the thermal response of the cold-worked specimen is compared to that of a virgin specimen. Although such methods also involve differences, those which incorporate a differential approach can eliminate a certain degree of systematic errors. However, since measurements in such techniques are taken after the deformation, they could not account for the stored energy that may be released immediately after the deformation. Further, in applications to fatigue, while U_c may in principle be obtained with this technique, it could not be used to monitor the accumulation of U of a component in service.

In this light, the Single-step approach is adopted in this current work, with the realization that precise measurements of both $\dot{W}$ and $\dot{Q}$ are necessary. While $\dot{W}$ may be easily and accurately determined from load-displacement data, accurate measurements of $\dot{Q}$ are much more difficult to achieve. Most existing experimental methods are based either on the use of an electrically heated calibration-specimen for matching the temperature measurements with those of the actual fatigue specimen (e.g., [5],[8],[10]), or by direct calculation of the heat passing out of the specimen from temperature measurements either on or outside of the specimen gage section (e.g., [6], [7] and [11]). However, all these methods require elaborate experimental setups and cannot adequately account for any transient effects. Indeed, most of the above-mentioned works were careful in stating that steady state conditions are required.

Rantsevich and Franyuk [12] proposed an experimental/analytical solution for calculating the thermal energy losses from a cyclically loaded specimen. It was shown that by knowing temperatures at two locations on a specimen, the steady-state diffusion equation may be solved for the source term by assuming symmetry and isothermal boundary conditions. In a later paper [13], Rantsevich established conditions for steady and quasi-steady assumptions so that certain transient problems may be solved incrementally. However, the restrictions on symmetry and isothermal conditions appear too severe and would not be applicable in real tests.

In this paper, a hybrid numerical/experimental technique for determining the heat dissipated by a cyclically loaded specimen is presented. Treated as an inverse problem, the one-dimensional diffusion equation is solved for the source term numerically. The customary boundary conditions used in the direct problems are replaced by a least squares criterion on the numerical temperature profile to fit the measured temperature profile at discrete time intervals. A stable scheme is formulated using the method of Lagrange multipliers and finite difference approximations. Because this method is independent of the temperature boundary conditions and thus the amount of heat escaped via the grips, standard testing equipment may be used with only minimal requirement for insulating the test section of the specimen to prevent convective heat loss.

NUMERICAL PROCEDURE

In general, the temperature field of a solid body under load is a function of the deformation state and the presence of any internal and external heat source and/or sink. The coupling between temperature and deformation is attributed to the thermoelastic effect, and the representation of plastic energy as internal heat sources. Because our interest is in the temperature variation from cycle to cycle, and not on its fluctuation within each cycle, the heat transfer problem can be greatly simplified by considering temperatures which are averaged over one complete cycle. Since the specimens under consideration are thermally insulated round bars which may be considered thermally thin (Biot numbers $<< 1$), the thermal response may be described by the one-dimensional diffusion equation:

$$\frac{\partial \theta}{\partial t} - \alpha \frac{\partial^2 \theta}{\partial x^2} = \frac{q}{\rho C} \tag{2}$$

where

θ = temperature averaged over one cycle (K),

$\alpha = \{k/\rho C\}$ = thermal diffusivity (m^2/sec) ,

k = material heat conductivity (J/m-sec-K),

ρ = density (kg/m^3) ,

C = specific heat (J/kg-K),

q = heat generation rate (J/m^3-sec).

Equation (2) is usually solved as a direct problem in which given the source term q, the temperature field is solved subject to certain initial and boundary conditions. In the present problem, however, the objective is to find q $(=\dot{Q})$ such that the temperature field best fit the measured data. Because an analytical form of q is not expected, a numerical approach to this problem was adopted. Equation (2) may be rewritten in the Crank-Nicolson finite difference form [14], viz:

$$\frac{\theta_i^t - \theta_i^{t-1}}{\Delta t} - \frac{\alpha}{2\Delta x^2}(\theta_{i+1}^t - 2\theta_i^t + \theta_{i-1}^t + \theta_{i+1}^{t-1} - 2\theta_i^{t-1} + \theta_{i-1}^{t-1}) = \frac{q}{\rho C}, \tag{3}$$

where the subscript i and superscript t indicate positional and temporal locations respectively, Δx is the linear mesh size, and Δt is the time-marching interval. Since the range of strains considered are much lower than those necessary to cause necking, uniform plastic deformation is expected. Hence, the heat source q (averaged over Δt) is assumed to be a function of time only.

Equation (3) may be rewritten as

$$\theta_{i-1}^t + A\theta_i^t + \theta_{i+1}^t = Bq + C_i, \tag{4}$$

in which

$$A = -2\left[1 + \frac{\Delta x^2}{\alpha \Delta t}\right],$$

$$B = -2\frac{\Delta x^2}{\alpha},$$

$$C_i = -\theta_{i-1}^{t-1} + 2\left[1 - \frac{\Delta x^2}{\alpha \Delta t}\right]\theta_i^{t-1} - \theta_{i+1}^{t-1}.$$

We now need to define an objective function for which q may be solved given some measured temperature data. An obvious choice is a least-squares criterion on the difference between measured and computed temperature profiles. At time t, let there be measured temperatures T_j at nodes j. The solution q is one which minimizes

$$S = \sum_j (T_j - \theta_j)^2. \tag{5}$$

That is, the solution must satisfy

$$\frac{\partial S}{\partial q} = 0, \text{ and } \frac{\partial^2 S}{\partial q^2} > 0. \tag{6}$$

One apparently straightforward approach would be to solve Eqs. (4-6) iteratively by the algorithm listed below.

1. Assume an initial value for q.
2. Solve for the temperature field directly.
3. Evaluate S using Eq. (5), and estimate q such that (6) will be satisfied.
4. Repeat steps 2 and 3 until Eq. (6) is satisfied within some specified tolerance.

However, this is relatively inefficient. Furthermore, the solution of Eq. (4) requires the assignment of temperature boundary conditions. Although other researchers have assumed either adiabatic or isothermal boundary conditions for solving similar direct problems (e.g., [2],[3]), it was apparent in our preliminary tests that neither assumption is valid. One alternative would be to use the measured values as boundary conditions. However, this would impose unnecessary bias to the end points, implying no measurement errors at these locations.

The above problems may be overcome by using the method of Lagrange multipliers. Treating Eq. (4) as constraints to the minimization of Eq. (5), we write the function X:

$$X = \sum_i [(T_i - \theta_i)^2 \delta_i + \lambda_i(\theta_{i-1} + A\theta_i + \theta_{i+1} - Bq - C_i)], \tag{7}$$

where

$$\delta_i = \begin{cases} 1 & \text{when } T_i \text{ exists,} \\ 0 & \text{when } T_i \text{ does not exist} \end{cases}$$

and

λ_i = Lagrange multipliers.

Note that θ_i is defined so that measured data T_i are not required for all i. For the solution to exist, we require

$$\frac{\partial X}{\partial \lambda_i} = 0 \qquad i = 2 \ldots N-1,$$

$$\frac{\partial X}{\partial \theta_i} = 0 \qquad i = 1 \ldots N, \tag{8}$$

$$\frac{\partial X}{\partial q} = 0.$$

The expansion of Eqs. (8) results in the following linear set of equations:

$$\left[\begin{array}{ccccccc|ccccccc|c}
1 & A & 1 & & & & & & & & & & & & -B \\
 & 1 & A & 1 & & & & & & & & & & & \cdot \\
 & & \cdot & \cdot & \cdot & & & & & & & & & & \cdot \\
 & & & \cdot & \cdot & \cdot & & & & & & & & & \cdot \\
 & & & & \cdot & \cdot & \cdot & & & & & & & & \cdot \\
 & & & & & 1 & A & 1 & & & & & & & -B \\
\hline
2\delta_1 & & & & & & & & 1 & & & & & & \\
 & 2\delta_2 & & & & & & & A & 1 & & & & & \\
 & & 2\delta_3 & & & & & & 1 & A & 1 & & & & \\
 & & & \cdot & & & & & & \cdot & \cdot & \cdot & & & \\
 & & & & \cdot & & & & & & \cdot & \cdot & \cdot & & \\
 & & & & & \cdot & & & & & & 1 & A & 1 & \\
 & & & & & & \cdot & & & & & & 1 & A & \\
 & & & & & & & 2\delta_N & & & & & & 1 & \\
\hline
 & & & & & & & & 1 & 1 & \cdot & \cdot & \cdot & 1 &
\end{array}\right]
\left\{\begin{array}{c}
\theta_1 \\ \theta_2 \\ \cdot \\ \cdot \\ \theta_{N-1} \\ \theta_N \\ \hline \lambda_2 \\ \lambda_3 \\ \cdot \\ \cdot \\ \cdot \\ \cdot \\ \lambda_{N-1} \\ q
\end{array}\right\}
=
\left\{\begin{array}{c}
C_2 \\ C_3 \\ \cdot \\ \cdot \\ \cdot \\ C_{N-1} \\ \hline 2\delta_1 T_1 \\ 2\delta_2 T_2 \\ \cdot \\ \cdot \\ \cdot \\ \cdot \\ 2\delta_N T_N \\ 0
\end{array}\right\} \tag{9}$$

where all blank spaces of the above matrix are zeros. Noting from Eq. (9),

$$2\,\delta_1\theta_1 + \lambda_2 = 2\delta_1 T_1$$

$$2\,\delta_N\theta_N + \lambda_{N-1} = 2\delta_N T_N \tag{10}$$

and with the solution region confined to the section bounded by the two outermost RTDs, so that

$$\delta_1 = \delta_N = 1 \tag{11}$$

we have

$$\theta_1 = T_1 - \frac{\lambda_2}{2}, \tag{12}$$

$$\theta_N = T_N - \frac{\lambda_{N-1}}{2}.$$

Substituting Eq. (12) into Eq. (9) results in

$$[M]\{x\} = \{y\}, \tag{13}$$

where

$$[M] = \left[\begin{array}{ccccccc|cccccc|cc}
A & 1 & & & & & & -1/2 & & & & & & -B \\
1 & A & 1 & & & & & & & & & & & \cdot \\
 & \cdot & \cdot & \cdot & & & & & & & & & & \cdot \\
 & & \cdot & \cdot & \cdot & & & & & & & & & \cdot \\
 & & & & 1 & A & 1 & & & & & & & \cdot \\
 & & & & & 1 & A & & & & & & -1/2 & -B \\
\hline
2\delta_2 & & & & & & & A & 1 & & & & & \\
 & 2\delta_3 & & & & & & 1 & A & 1 & & & & \\
 & & \cdot & & & & & & \cdot & \cdot & \cdot & & & \\
 & & & \cdot & & & & & & \cdot & \cdot & \cdot & & \\
 & & & & \cdot & & & & & & 1 & A & 1 & \\
 & & & & & 2\delta_{N-1} & & & & & & 1 & A & \\
 & & & & & & \cdot & 1 & 1 & \cdot & \cdot & \cdot & 1 &
\end{array}\right] \tag{14a}$$

$$\{x\} = \left\{\begin{array}{c} \theta_2 \\ \theta_3 \\ \cdot \\ \cdot \\ \theta_{N-1} \\ \hline \lambda_2 \\ \cdot \\ \cdot \\ \lambda_{N-1} \\ q \end{array}\right\}, \tag{14b}$$

$$\{y\} = \left\{\begin{array}{c} C_2 - T_1 \\ C_3 \\ \cdot \\ \cdot \\ C_{N-1} - T_N \\ \hline 2\delta_2 T_2 \\ 2\delta_3 T_3 \\ \cdot \\ \cdot \\ 2\delta_{N-1} T_{N-1} \\ 0 \end{array}\right\}. \tag{14c}$$

The solution for θ_i and q may thus be obtained by solving Eq. (13) for **x**.

A FORTRAN program was developed for solving Eq. (13) on a 16 bit microcomputer. The sparseness of the matrix [*M*] was not exploited, and Gaussian elimination was used in its inversion for sake of simplicity. Double precision was used throughout, and the conditioning of [*M*] was checked and found to be satisfactory. A uniform mesh of 16 intervals was used for the 40 mm (1.575 in.) gage section of the specimen. This was selected so that the measured temperature locations are coincident with the finite difference nodes. A marching time step was set at 0.2 times the interval for

which experimental data were available. For the 1 Hz tests, this was equivalent to a time step of 0.2 sec for the first 50 seconds, and then 2 seconds thereafter. The required measured values (T_i) between data points were obtained by interpolation. Mesh refinements were performed on several runs and the selected meshes were found to be adequate.

EXPERIMENTAL PROCEDURE

Testing

The tests were performed under fully reversed sinusoidal uniaxial loading in a closed loop servohydraulic testing machine operated in strain control. Two frequencies (1 Hz, 4 Hz) were considered. Temperature and load-strain data were obtained continuously for the first fifty cycles and for every tenth cycle thereafter. Alignment of the cross heads was check before each test. A block schematic of the testing setup and associated instrumentation is shown in Fig. 1. A microcomputer was used to control the test and instrumentation.

Specimens were 15.88 mm (.625 in.), and 19.05 mm (.75 in.) diameter off the shelf bar stock aluminum 6061 − T6. No machining or specimen polishing was performed before testing. Specimen length from grip to grip was approximately 63.5 mm (2.5 in.) and the strain was measured over a 50.8 mm (2.0 in.) gage length. Prior to each test, the thermal connection of the temperature measuring devices was examined by applying an external heat source to the bar on one end and determining the resulting internal source term q numerically. Since there was actually no internal source, q should be vanishing. For all cases the internal source term obtained was less than 0.01 MW/m^3 (0.268 BTU/ft^3-sec), and the mean standard error of the measured temperature from the numerically calculated value was less than 0.01 K. This was considered satisfactory as the manufacturer's specification on the RTD accuracy was of this order.

Temperature Profile Measurement

The temperature profile of the specimen was measured by 9 platinum resistance temperature detectors (RTDs). The dimensions of the RTDs were 2.3 mm × 2 mm and 1 mm thick (0.091 in × 0.079 in. × 0.039 in.). For the range of temperatures measured there exists a linear relation between resistance and temperature [15] given by

$$R = 0.385\,T + 100, \tag{15}$$

where

T = temperature (°C),

R = resistance (Ω).

The 9 RTDs were placed over a 40 mm (1.575 in.) length, and a thin layer of silicone paste was used to ensure good thermal contact with the specimen. The thermal conductivity of the paste was extremely high i.e. 140 J/m-sec-K (16 BTU-in/hr-ft^2-°F) [16]. The position and the scan sequence for the RTDs for both frequencies are shown in Figs. 2a and 2b. To minimize convection losses, the specimen was wrapped with fiberglass insulation.

The resistance of the RTDs was determined by using 4-wire ohm measurements. The temperature data were obtained by an integrated data acquisition unit (DAU # 1) consisting of a 6.5 digit integrating voltmeter, a 20 channel FET multiplexer with a maximum scan rate of 5500 channels/sec, a counter with a resolution of 1 μsec, and memory storage. The integration time for each voltage measurement was 0.1 power line cycle (60 Hz). The RTDs were-scanned in sequential order as shown in Fig. 2a, 2b to minimize bias toward one end.

Since the integration time was shorter than the completion of a 60 Hz cycle, the measurements obtained were susceptible to power line noise. Therefore, a sampling rate was chosen to capture the alternate rise and fall of the 60 Hz noise and its effect could thus be eliminated upon averaging. This may be optimized by setting the sampling interval for each channel to $(N + 1/2) \cdot T_p$, where N is an integer, and T_p is the period of the power line noise. With the available equipment, $N = 2$ was chosen to give a maximum sampling rate of 24 scans/sec for 1 Hz and 6 scans/sec for 4 Hz.

Measurement of Hysteresis Energy

The hysteresis energy is given by the cyclic integral of the engineering stress and strain. The load and strain data were obtained by a separate data acquisition unit (DAU #2) with two high speed A/D 12 bit voltmeters and a high speed memory storage. The load range was set so that 9000 N (2000 lb_f) corresponded to a 1 volt output signal. The strain data were obtained with an extensometer with a 50.8 mm (2.0 in.) gage length and calibrated so that a 1 volt output signal corresponded to 0.4% strain. Fifty data points per cycle were taken and the voltmeters were triggered by an external pulse occurring at the beginning of each cycle from a function generator driving the test (see Fig. 1). The start of cycle pulses were also recorded by a counter contained in DAU # 2. The data were stored in memory and later transferred to a computer for calculation of the hysteresis energy by numerical integration.

System Time Constant

The RTD response may be described by as a first order system and thus exhibits a time lag to an external stimulus. The system time constant was determined by attaching a RTD to a specimen similar to those to be tested, and examining its response to an applied cycling elastic load. The thermoelastic response of the specimen may be predicted from Kelvin's law for adiabatic conditions

$$\Delta T = -KT\,\Delta\sigma_{ii}, \tag{16}$$

where

$\Delta\sigma_{ii}$ = cyclic amplitude of the first invariant of stress (N/m^2),

K = thermoelastic constant (m^2/N),

T = absolute temperature (K),

ΔT = cyclic temperature amplitude (K).

The time constant τ may be determined from the measured amplitude and the amplitude predicted by Kelvin's law

$$\tau = \frac{1}{\Omega}\sqrt{(T_E/T_M)^2 - 1} \tag{17}$$

where

T_M = measured response (K),

T_E = predicted thermoelastic response (K),

Ω = excitation frequency (sec^{-1}).

The time constant may also be obtained independently by examining the phase lag ϕ between the applied load and the thermoelastic response signals as given by

$$\tau = \frac{1}{\Omega}\tan\phi. \tag{18}$$

Using a lock-in-amplifier to measure the amplitude and the phase lag of the thermoelastic response, the time constant was determined to be less than 0.2 sec. by both equations 17 and 18. Numerical simulations indicated that such time response had no significant influence on the determination of the heat conversion efficiency for the tests considered.

RESULTS AND DISCUSSION

Simulated Tests

To test the inverse diffusion solution scheme, a direct problem was first constructed and solved using the Crank-Nicolson finite difference scheme. Various fictitious, but representative, time-dependent heat source terms, as well as asymmetric time-dependent Dirichlet boundary conditions were tested. At 1 sec intervals, the temperatures at the 9 corresponding RTD positions were extracted from the direct solutions. To simulate actual experimental data, two types of errors were added to the numerical outputs. Systematic errors were simulated by a ($< \pm$ 0.1 K) random offset fixed for each RTD throughout the run and random errors associated with instrumentation noise were modeled by a $< \pm 0.1$ K signal updated at each time increment.

The simulated RTD data were then used as input data in the inverse program. After several runs, it was found that the absolute errors in the computation of $\dot{Q}$ were relatively independent of $\dot{Q}$. This means that the relative accuracy would improve with increases in $\dot{Q}$. It was also noticed that while the random noise determined the size of the scattering of $\dot{Q}$ about the mean from increment to increment, the random offsets produced a scatter of the mean about zero from run to run (given different seeds for the random errors). From these runs, it was found that for the material chosen, and the above specified temperature measurement errors, $\dot{Q}$ may be determined from the inversion program to the order of 0.01 MW/m^3 (0.268 BTU/ft^3-sec).

Actual Tests

The results of the simulated runs effectively established the resolution of our proposed inverse scheme and helped in deciding on the strain ranges suitable in the actual fatigue tests. Since the heat dissipated was expected to be near the hysteresis energy, the strain ranges: $\pm 0.522\%$ to $\pm 0.773\%$ at 1 Hz and $\pm 0.375\%$ to $\pm 0.571\%$ at 4 Hz were selected to ensure a hysteresis energy rate of at least of the order of 1 MW/m^3 (26.75 BTU/ft^3-sec).

All tests were run to complete fracture. Since the bar stock specimens lacked any transitional section, fracture occurred invariably at the first grip indentation of one of the grips. No apparent preference to either the fixed or moving grip was noticed. Results for a typical 1 Hz run and 4 Hz run are shown in Figs. 3-12. Figures 3 and 4 show the development of both measured and computed temperatures at the center and ends. Temperature profiles at three different times are also shown in Figs. 5 and 6. It can be seen that excellent agreements between the experimental and computed temperature profiles were achieved. The mean standard error (MSE) was calculated at each increment, and for all the specimens tested, the maximum MSE ranged from 0.02 K to 0.16 K. Such exceptional agreement validates the assumption of uniform heat dissipation along the length of the specimen, and reinforces confidence in its solution.

The general rise of the end RTD readings warrants some comments on the treatment of boundary conditions by other analytical and numerical models. When solving the direct problem, most assume isothermal boundary conditions based on the argument that the grips act as infinite heat sinks. However, it is clear from our measurements (extrapolating to the grips located at approximately 10 mm from the end RTD's) that such assumptions are not valid. No such assumptions were made in the present analysis.

Another interesting feature of the temperature histories is the rapid rise of temperature at one end relative to the other just prior to failure. The fact that this hotter end was found always to be the fractured end suggests that this rapid increase must be associated with the initiation and subsequent growth of the crack since the intense crack-tip plastic deformation acted as a large external (i.e., outside the gage length) heat source. It is interesting to note that in a series of fatigue tests on steel, Rantsevich [13] showed that by analyzing temperature data near the "vulnerable zone," the detection of crack initiation can in fact be made much earlier than the magnetic method used in his tests.

Figures 7 and 8 show the comparison of the computed values of $\dot{W}$ and $\dot{Q}$. For all cases studied, the energy rates showed three distinctive regimes: a brief but rapid developing segment at the start, followed by a steady intermediate region and finally another rapidly changing section prior to complete fracture. The appearance of these three regimes was also found by Haigh [6], who referred to them as the primary, secondary and tertiary stages, and attributed the behavior as a material characteristic. However, after careful examination of the strain histories from the current tests, we concluded that this was more closely associated with the characteristics of the testing machine. Despite testing under strain control, the testing machine used was unable to maintain a strictly constant strain, particular at the higher frequency (4 Hz). Even for the 1 Hz tests where the strain history appeared relatively constant, a plot of the square of the strain history (since near the elastic limit, the hysteresis energy is roughly proportional to the square of the strain) revealed the three distinct stages resembling those of the hysteresis history.

The fact that the hysteresis level was not maintained constant throughout the tests posed no great problem to our present analysis as steady state conditions were not required. In general, $\dot{Q}$ was found to range between 85% to 95% of $\dot{W}$. Invariably, the heat conversion efficiency, defined as $\dot{Q}/\dot{W}$, started at a lower level and then gradually rose to a level or near-level plateau (see Figs. 9 and 10).

At first, this was thought to be due to an insufficient RTD time response rate. However, an analysis based on the measured time constants (see experimental procedure) showed this effect to be negligible. Another indication of a sufficient response time was the fact that there was a good correlation between the fluctuations of $\dot{W}$ and $\dot{Q}$ during the transient state (see inset in Fig. 8). Since $\dot{W}$ and $\dot{Q}$ were obtained by independent means, such good correlation also serves to support the correctness in the calculation of $\dot{Q}$. The results therefore suggest that the absorption of energy (U) is greatest at the beginning of test, and thus confirming the notion that the accumulation of damage is greatest at the start of cycling. For most cases, $\dot{Q}$ diverged from $\dot{W}$ in the tertiary stage. The direction of divergence (i.e., whether $\dot{Q} < \dot{W}$ or $\dot{W} < \dot{Q}$) appeared unpredictable. Since this tertiary stage invariably corresponded to the divergence of the end RTD readings, indicating crack initiation and propagation, increasing bending must have been present so that the extensometer data could not have truly represented the average strain of the specimen. This in turn would have led to an erroneous calculation of $\dot{W}$. Because of the uncertainty in the determination of $\dot{W}$ in this region, it was decided to exclude it from the current analysis. In other words, we define failure to be the moment at which sub-critical crack growth becomes detectable as opposed to the more conventional definition of gross specimen fracture. For our test results, this corresponded to the time at which one end RTD reading diverged from the other.

The total hysteresis energy W_c and the total absorbed energy U_c up to the point of crack initiation N_c for all the specimens considered are presented in Fig. 11. While W_c shows a high dependency on N_c, U_c appeared to be relatively constant over the cycle range tested. However, in order to confidently establish that U_c is a strict constant, more tests are needed where a broad cycle range is considered and the scatter reduced. The use of higher frequency loads would permit the heat dissipated to be measured at lower loads and thus higher N_c. The use of properly designed specimens (as opposed to the round-bar stocks used in the present work), more temperature measurement stations along the specimen, as well as a more precise method for determining the moment of crack initiation would help in reducing the scatter seen in the present data.

CONCLUSION

A hybrid experimental/numerical method for determining the heat dissipated from a uniformly deforming specimen is presented. Both steady and non-steady problems can be handled with this technique, and it does not require any particular boundary temperature conditions to be specified. The method was applied in a study on the relationship between the irreversible work input and the heat dissipated for a number of aluminum 6061-T6 specimens under fatigue loading. Its accuracy is supported by the excellent agreement between measured and computed temperatures, and its performance during the initial transient stage is demonstrated by the good correlation between the fluctuations in the measured hysteresis power $\dot{W}$, and the heat dissipation rate $\dot{Q}$ which were obtained by independent means. It was found that $\dot{Q}$ ranged between 85% to 95% of $\dot{W}$ and the rate of energy absorbed by the material $\dot{U}$ was invariably greatest at the start of the tests, inferring an initially higher rate of damage accumulation. The summing of energies up to the point of crack initiation revealed that while W_c varied greatly with N_c, the total energy accumulated U_c appeared relatively invariant over the range of cycles considered. However, to adequately address the issue on whether U_c is a material parameter, more tests are needed for different loading conditions and higher number of cycles to failure.

ACKNOWLEDGEMENTS

The authors would like to acknowledge the helpful discussions and suggestions of their collegues Dr. Peter Matic, Virginia DeGiorgi, Robert Badaliance and Mr. Dan Harvey of the Mechanics of Materials Branch. The authors would also like to extend their gratitude to Mr. Clark Welsh of Geo-Centers for his assistance in the experiments. Finally, a special acknowledgement is reserved for Prof. Mitchell Jolles of Wiedner University who first suggested this study.

REFERENCES

1. Fortes, M.A. "The Effect of Strain Rate on the Stored and Dissipated Energies of Cold Work in Tension," Scripta Metallurgica, Vol. 7, pp. 549-552, 1977.

2. Korhonen, A.S. and Kleemola, H.J "Effects of Strain Rate and Deformation Heating in Tensile Testing," Metal. Trans. A, Vol. 9A, pp. 979-986, 1978.

3. Gao, Y. and Wagoner, R.H. "A Simplied Model of Heat Generation During the Uniaxial Tensile Test," Metal. Trans. A, Vol. 18A, pp. 1001-1009, 1987.

4. Thomson, W. (Lord Kelvin) *Mathematical and Physical Papers*, Vol. 3, C.J. Clay and Sons, 1890.

5. Hopkinson, B. and Williams, G.T. "The Elastic Hysteresis of Steel," Proc. Roy. Soc. London, Vol. 87, pp. 10-15, 1912.

6. Haigh, B.P. "Hysteresis in Relation to Cohesion and Fatigue," Trans. Faraday Soc. Vol. 24, pp. 125-127, 1928.

7. Gurevich, S.E. and Gaevoi, A.P. "Method of Experimentally Determining Rupture Energy in Cyclical (Fatigue) Loading," Zavodskaya Laboratoriya, Vol. 39, pp. 1110-1114, 1973.

8. Romashov, R.V. and Fedorov, V.V. "Method of Experimentally Checking Thermodynamic Ideas on the Failure of a Solid Body During Fatigue Tests," Zavodskaya Laboratoriya, Vol. 41, pp. 229-232, 1975.

9. Bever, M.B., Holt, D.L., and Titchener, A.L "The Stored Energy of Cold Work," Progress in Materials Science, Vol. 17, Pergamon Press, 1973.

10. Btotny, R. and Kaleta, J. "A Method for Determining the Heat Energy of the Fatigue Process in Metals Under Uniaxial Stress," Int. J. Fatigue, Vol. 8, pp. 29-33, 1986.

11. Harry, R., Joubert, F. and Gomma, A. "Measuring the Actual Endurance Limit on One Specimen Using a Nondestructive Method," J. Eng. Matl. and Tech., Vol. 103, pp. 71-76, 1981.

12. Rantsevich, V. B. and Franyuk, V. A. "Calculation of the Steady-State Temperature Field and Thermal Energy Losses in Samples Undergoing Fatigue," Problemy Prochnosti, Vol. 1, pp. 102-104, 1976.

13. Rantsevich, V.B. "Thermal Detection of Cracks in Fatigue Testing of Parts," Defektoskopiya, Vol. 5, pp. 102-108, 1977.

14. Omega Engineering Inc., *Complete Temperature Measurement Handbook and Encyclopedia*, p. T-81, 1986.

15. Ibid, J.-5.

Appendix A

```
      PROGRAM TSOLVE
C
C     program for solving the inverse 1-D diffusion equation.  Given
C     temperature readings at at least three distinct locations on a
C     fatigue specimen, the heat source is solved and compared to the
C     the amount of irreversible work generated.
C
      IMPLICIT REAL*8 (A-H,O-Z)
      PARAMETER(MMAX=100, MXMAX=50, MTMAX=10)
      DIMENSION X(MMAX,MMAX), Y(MMAX), RHS(MMAX)
      DIMENSION XINV(MMAX,MMAX), AUX(MMAX,MMAX)
      DIMENSION THETA(MXMAX)
      DIMENSION XT(MXMAX),JT(MXMAX),JTX(MXMAX)
      DIMENSION CC(MXMAX)
      DIMENSION T(MTMAX), T1(MTMAX), T2(MTMAX), T3(MTMAX)
      DIMENSION TEMP1(MTMAX),TEMP2(MTMAX),TEMP3(MTMAX)
      DIMENSION AT(MTMAX), BT(MTMAX), CT(MTMAX)
      COMMON //TAU, DELAY(MTMAX)
      CHARACTER*79 LINE
      CHARACTER*15 INFIL1, INFIL2, INFIL3

      WRITE(*,'(1X,42HENTER SOLUTION-SPECIFICATIONS FILE NAME:  , $)')
      READ(*,'(A)') INFIL1

      WRITE(*,'(1X,42HENTER TEMPERATURE-MEASUREMENTS FILE NAME: , $)')
      READ(*,'(A)') INFIL2

      WRITE(*,'(1X,42HENTER HYSTERYSIS FILE NAME:               , $)')
      READ(*,'(A)') INFIL3

      OPEN(UNIT=1,FILE=INFIL1,STATUS='OLD')
      READ(1,'(A79)') LINE
      READ(1,*) NDT,NDX,XL,XK,RHO,CV
      WRITE(*,'(/,1X,A79)') LINE
      WRITE(*,'(3X,I4,6X,I4,4X,4G10.3)') NDT,NDX,XL,XK,RHO,CV
      READ(1,'(A79)') LINE
      READ(1,*) NRTD
      WRITE(*,'(/,1X,A)') 'NUMBER OF TEMPERATURE MEASUREMENT POINTS'
      WRITE(*,'(1X,I4)') NRTD
      READ(1,'(A79)') LINE
      READ(1,*) (XT(I),I=1,NRTD)
      WRITE(*,'(/,1X,A79)') LINE
      WRITE(*,'(1X,8G10.3)') (XT(I),I=1,NRTD)
      READ(1,'(A79)') LINE
      READ(1,*) TSTART
      WRITE(*,'(/,1X,A79)') LINE
      WRITE(*,'(1X,G10.3)') TSTART
      READ(1,'(A79)') LINE
      READ(1,*) TPULSE, (DELAY(I),I=1,NRTD)
      WRITE(*,'(/,1X,A79)') LINE
      WRITE(*,'(1X,8G10.3)') TPULSE, (DELAY(I),I=1,NRTD)
      WRITE(*,*)

      NT=NDX+1
      MX=2*NT-3
C
C-----NDT number of time-marching steps between hysterysis data interval
C-----NDXnumber of mesh intervals along the solution length
C-----XLlength of specimen
C-----XKcoefficient of thermal conduction
C-----RHOdensity of the material
C-----CVspecific heat under constant volume
C-----NRTDnumber of rtd stations
C-----TSTARTsolution starting time
C-----NTnumber of finite difference nodes
C-----MX        size of the solution matrix
C
      IF(MX .GT. MMAX .OR. NT .GT. MXMAX .OR. NRTD .GT. MTMAX) THEN
        WRITE(*,'(A,A/A)') ' *** INSUFFICIENT MEMORY SPACE ALLOCATED, ',
     +  'CHECK ARRAY DECLARATIONS ---',' PROGRAM TERMINATED ! ***'
        STOP
      ENDIF

C
C-----calculate grid positions where temperature measurements are available
C
      IF(NRTD .LT. 3 .OR. NRTD .GT. MTMAX) THEN
        WRITE(*,10)
10      FORMAT(/' INVALID NUMBER OF TEMPERATURE MEASUREMENTS,',/
     +          ' PROGRAM TERMINATED!')
        STOP
      ENDIF
C
C-----convert dx, xl and xt to metres, and delay(i) to time units
```

```
C
      DX=0.001*DX
      XL=0.001*XL
      DO 20 I=1,NRTD
        XT(I)=0.001*XT(I)
        DELAY(I)=TPULSE*DELAY(I)
20    CONTINUE
C
C-----check whether the rtds are located sufficiently close to the FD nodes
C
      DX=XL/FLOAT(NDX)
      DO 510 I=1,NRTD
        XJT=XT(I)/DX+1
        FRACTXJT=XJT-INT(XJT+0.001)
        IF(ABS(FRACTXJT) .GT. 0.001) THEN
          WRITE(*,'(/A,I2,A)') ' *** WARNING ***, RTD-',I,' DOES NOT ',
     +    'LIE EXACTLY ON A GRID POINT !'
          X1=(INT(XJT-0.5)-1)*DX
          JT(I)=INT(XJT-0.5)+INT((XJT-X1)/DX+0.5)
        ELSE
          JT(I)=INT(XJT+0.001)
        ENDIF
510    CONTINUE

      OPEN(UNIT=2,FILE=INFIL2,STATUS='OLD')
      OPEN(UNIT=3,FILE=INFIL3,STATUS='OLD')
      OPEN(UNIT=4,FILE='TSOLVE.RES',STATUS='NEW')
C
C-----obtain first three rtd measurements
C
      T1(1)=0.
      DO 42 I=1,NRTD
        TEMP1(I)=0.
42    CONTINUE
C
45    READ(2,*) T2(1), (TEMP2(I), I=1,NRTD)
      IF(TSTART .GT. T2(1)) THEN
        T1(1)=T2(1)
        DO 46 I=1,NRTD
          TEMP1(I)=TEMP2(I)
46      CONTINUE
        GOTO 45
      ENDIF
      READ(2,*) T3(1),(TEMP3(I),I=1,NRTD)
      DO 48 I=1,NRTD
        T1(I)=T1(1)+DELAY(I)
        T2(I)=T2(1)+DELAY(I)
        T3(I)=T3(1)+DELAY(I)
48    CONTINUE
C
C-----read in time and hysterysis rate
C
      TAU1=0.
      IF(TSTART .NE. 0.) THEN
50      CONTINUE
          READ(3,*) TAUMID, HYST
          TAU2=2.*(TAUMID-TAU1)
          IF((TSTART-TAU1) .GT. 0.00001) THEN
            TAU1=TAU2
            GOTO 50
          ENDIF
        CONTINUE
        CALL GETRTD(T,T1,T2,T3,TEMP1,TEMP2,TEMP3,AT,BT,CT,NRTD)
        CALL FITPROF(TEMP1,XT,NRTD,THETA,NT,DX)
      ENDIF
C
      DT0=0.
      TAU=TAU1
      B=-2.*DX*DX/XK
      ALPHA=XK/(RHO*CV)
      QSUM=0.
      WSUM=0.
      DTHMAX=0.
C
C-----HYSThysterysis energy rate during the period between the
C      tau1 and tau2
C-----QSUMtotal heat dissipated
C-----WSUMtotal irreversible work
C
100   CONTINUE
      Q=0.
      ERRSUM=0.
C
      READ(3,*,END=1000) TAUMID, HYST
```

```
      TAU2=2.*TAUMID-TAU1
C
      DTAU=TAU2-TAU1
      DT=DTAU/FLOAT(NDT)
      IF(ABS((DT-DT0)/DT) .GT. 0.001) THEN
        A=-2.*(1+DX*DX/(ALPHA*DT))
        C=2.*(1.-DX*DX/(ALPHA*DT))
C
C-------invert matrix
C
        IF(TAU1 .NE. TSTART) THEN
          WRITE(*,'(/A/)') ' CHANGE IN DT, RE-INVERTING MATRIX ....'
        ELSE
          WRITE(*,'(/A/)') ' INVERTING MATRIX ....'
        ENDIF
        CALL FILLMAT(A,B,MX,MMAX,NRTD,X,JT)
        CALL MATINV(MMAX,MX,X,XINV,AUX)
      ENDIF
C
      DO 700 JDT=1,NDT
        TAU=TAU+DT
C
C-------interpolate rtd readings at tau
C
        CALL GETRTD(T,T1,T2,T3,TEMP1,TEMP2,TEMP3,AT,BT,CT,NRTD)
C
C-----
C
        DO 620 I=2,NT-1
          CC(I-1)=C*THETA(I)-THETA(I-1)-THETA(I+1)
620     CONTINUE
C
C-------fill rhs
C
        CALL FILLRHS(NT,MX,NRTD,CC,RHS,JT,T)
C
C-------calculate new temperatures and q
C
C-------THETAcalculated temperatures
C
        DO 640 I=1,NT-2
          THETA(I+1)=0.
          DO 630 J=1,MX
            THETA(I+1)=THETA(I+1)+XINV(I,J)*RHS(J)
630       CONTINUE
640     CONTINUE
        XLAM2=0.
        XLAMM=0.
        QDOT=0.
        DO 650 J=1,MX
          XLAM2=XLAM2+XINV(NT-1,J)*RHS(J)
          XLAMM=XLAMM+XINV(MX-1,J)*RHS(J)
          QDOT =QDOT +XINV(MX  ,J)*RHS(J)
650     CONTINUE
        Q=Q+QDOT*DT
C
        THETA(1) =T(1)-   0.5*XLAM2
        THETA(NT)=T(NRTD)-0.5*XLAMM
C
C-----calculate degree of error in temperature measurements
C
      DO 680 I=1, NRTD
        DTH=THETA(JT(I))-T(I)
        IF(ABS(DTH) .GT. DTHMAX) DTHMAX=ABS(DTH)
        ERRSUM=ERRSUM+DTH*DTH
680   CONTINUE

700   CONTINUE
      ERRSUM=ERRSUM/(NDT*(NRTD-2))
      ERRSTD=SQRT(ERRSUM)
      QSUM=QSUM+Q
      WSUM=WSUM+HYST*DTAU
      ETA=Q/(HYST*DTAU)
      USUM=WSUM-QSUM
      WRITE(*,'(F10.2, 1X, F10.3, 4(1X,G10.3))') TAUMID, ETA, USUM,
     +      WSUM, DTHMAX, ERRSTD
      WRITE(4,'(1X,F10.2, 1X,F10.3, 4(1X,G10.3), 3X, 20(1H-))') TAUMID,
     +     ETA, USUM, WSUM, DTHMAX, ERRSTD
      WRITE(4,'(10(1X,F7.2))') TAU, (THETA(I), I=1,NT)
      WRITE(4,'(10(1X,F7.2))') (T(I), I=1,NRTD)
      TAU1=TAU
      DT0=DT
      GOTO 100
```

```
1000  CONTINUE
      AVETA=100.*(1.- USUM/WSUM)
      WRITE(4,'(/1X,A,G10.3,A)') 'TOTAL ACCUMULATED ENERGY = ',USUM,
     +       ' J/M^3'
      WRITE(4,'(/1X,A,G10.3,A)') 'AVERAGE WORK-HEAT CONVERSION EFFICIENC
     +Y = ', AVETA, ' %'
      WRITE(*,'(/1X,A,G10.3,A)') 'TOTAL ACCUMULATED ENERGY = ',USUM,
     +       ' J/M^3'
      WRITE(*,'(/1X,A,G10.3,A)') 'AVERAGE WORK-HEAT CONVERSION EFFICIENC
     +Y = ', AVETA, ' %'
      WRITE(*,'(/1X,A)') '*** RUN COMPLETED ***'
      STOP
      END

      SUBROUTINE GETRTD(T,T1,T2,T3,TEMP1,TEMP2,TEMP3,AT,BT,CT,NRTD)
C
C     Routine for interpolating the rtd readings.
C     Parabolic interpolation is used when data spacing is less than or equal
C     to 2 sec.  Otherwise, linear interpolation is used.
C
      IMPLICIT REAL*8 (A-H,O-Z)
      DIMENSION T(NRTD), T1(NRTD), T2(NRTD), T3(NRTD)
      DIMENSION TEMP1(NRTD), TEMP2(NRTD), TEMP3(NRTD)
      DIMENSION AT(NRTD), BT(NRTD), CT(NRTD)
      COMMON //TAU, DELAY(1)
      LOGICAL LINEAR
      DATA LINEAR /.FALSE./

      IF(TAU .GT. T3(1) .OR. (AT(1)+BT(1)+CT(1)) .EQ. 0.) THEN
        IF(TAU .GT. T3(1)+1.E-6) THEN
          DO 10 I=1,NRTD
            T1(I)=T2(I)
            T2(I)=T3(I)
            TEMP1(I)=TEMP2(I)
            TEMP2(I)=TEMP3(I)
10        CONTINUE
15        READ(2,*,END=1000) T3(1),(TEMP3(I),I=1,NRTD)
          IF(TAU .GT. T3(1)) GOTO 15
          DO 20 I=1,NRTD
            T3(I)=T3(1)+DELAY(I)
20        CONTINUE
        ENDIF
C
C-----re-evaluate polynomial coefficients
C
        IF(T3(1)-T2(1) .GT. 2.) THEN
          LINEAR=.TRUE.
          DO 25 I=1,NRTD
            BT(I)=(TEMP2(I)-TEMP3(I))/(T2(I)-T3(I))
            CT(I)=TEMP2(I)-BT(I)*T2(I)
25        CONTINUE
        ELSE
          LINEAR=.FALSE.
          DO 30 I=1,NRTD
            AT(I)=((T1(I)-T3(I))*(TEMP1(I)-TEMP2(I))-(T1(I)-T2(I))*
     +            (TEMP1(I)-TEMP3(I))) / ((T1(I)*T1(I)-T2(I)*T2(I))*
     +            (T1(I)-T3(I))-(T1(I)*T1(I)-T3(I)*T3(I))*
     +            (T1(I)-T2(I)))
            BT(I)=(TEMP1(I)-TEMP2(I)-AT(I)*(T1(I)*T1(I)-T2(I)*T2(I)))/
     +            (T1(I)-T2(I))
            CT(I)=TEMP1(I)-AT(I)*T1(I)*T1(I)-BT(I)*T1(I)
30        CONTINUE
        ENDIF
      ENDIF
C
C-----interpolate rtd readings
C
      IF(LINEAR) THEN
        DO 40 I=1,NRTD
          T(I)=BT(I)*TAU+CT(I)
40      CONTINUE
      ELSE
        DO 50 I=1,NRTD
          T(I)=AT(I)*TAU*TAU+BT(I)*TAU+CT(I)
50      CONTINUE
      ENDIF

      RETURN

1000  WRITE(*,*) ' END OF FILE IN READING RTD MEASUREMENTS'
      WRITE(*,*) ' PROGRAM TERMINATED !'
      STOP
      END
```

```
      SUBROUTINE FILLMAT(A,B,M,MMAX,NRTD,X,JT)
      IMPLICIT REAL*8 (A-H,O-Z)
      DIMENSION X(MMAX,MMAX)
      DIMENSION JT(NRTD)
C
      NT=(M+3)/2
      DO 500 I=1,M
        DO 510 J=1,M
          X(I,J)=0.
510     CONTINUE
500   CONTINUE

C
      X(1,1)=A
      X(1,2)=1.
      X(1,NT-1)=-0.5
      X(1,M)=-B
      DO 520 I=2,NT-3
        X(I,I-1)=1.
        X(I,I)=A
        X(I,I+1)=1.
        X(I,M)=-B
520   CONTINUE
      X(NT-2,NT-3)=1
      X(NT-2,NT-2)=A
      X(NT-2,M-1)=-0.5
      X(NT-2,M)=-B

      X(NT-1,NT-1)=A
      X(NT-1,NT)=1.
      DO 530 I=NT,M-2
        X(I,I-1)=1.
        X(I,I)=A
        X(I,I+1)=1.
530   CONTINUE
      X(M-1,M-2)=1.
      X(M-1,M-1)=A

      DO 540 I=NT-1,M-1
        X(M,I)=1.
540   CONTINUE
C      X(M,M)=2

      DO 550 I=2,NRTD-1
        X(NT+JT(I)-3,JT(I)-1)=X(NT+JT(I)-3,JT(I)-1)+2.
550   CONTINUE

      RETURN
      END

      SUBROUTINE MATINV(MMAX,M,A,AINV,AA)
      IMPLICIT REAL*8 (A-H,O-Z)
      DIMENSION A(MMAX,MMAX), AINV(MMAX,MMAX)
      DIMENSION AA(MMAX,MMAX)

C      PRINT*,'A='
C      DO 500 I=1,M
C        WRITE(*,'(1X,9G10.3)') (A(I,J),J=1,M)
C500   CONTINUE
      DO 510 I=1,M
        DO 520 J=1,M
          AINV(I,J)=0.
          AA(I,J)=A(I,J)
520     CONTINUE
        AINV(I,I)=1.
510   CONTINUE

      DO 530 K=2,M
        DO 540 I=K,M
          DO 550 KK=1,M
            AINV(I,KK)=AINV(I,KK)-AINV(K-1,KK)*(A(I,K-1)/A(K-1,K-1))
550       CONTINUE
          DO 560 J=K,M
            A(I,J)=A(I,J)-A(I,K-1)*(A(K-1,J)/A(K-1,K-1))
560       CONTINUE
540     CONTINUE
530   CONTINUE

      DO 570 KK=1,M
        AINV(M,KK)=AINV(M,KK)/A(M,M)
        DO 580 I=M-1,1,-1
          DO 590 J=I+1,M
            AINV(I,KK)=AINV(I,KK)-A(I,J)*AINV(J,KK)
590       CONTINUE
```

```
          AINV(I,KK)=AINV(I,KK)/A(I,I)
580     CONTINUE
570   CONTINUE
C
C      PRINT*,'A^-1='
C      DO 600 I=1,M
C        WRITE(*,'(1X,9G10.3)') (AINV(I,J),J=1,M)
C600   CONTINUE

      AMAX=0.
      DO 610 I=1,M
        DO 620 J=1,M
          ATEST=0.
          DO 630 K=1,M
            ATEST=ATEST+AA(I,K)*AINV(K,J)
630       CONTINUE
          IF(I .EQ. J) ATEST=ATEST-1.
          IF(ABS(ATEST) .GT. AMAX) AMAX=ABS(ATEST)
620     CONTINUE
610   CONTINUE
      IF(AMAX .GT. 1.E-10)
     +  WRITE(*,'(A)') '*** WARNING, MATRIX INVERSION MAY BE',
     +                 ' INACCURATE ***'
C       PRINT*,'I='
C       DO 640 I=1,M
C         WRITE(*,'(1X,9G10.3)') (A(I,J),J=1,M)
C640    CONTINUE
C
      RETURN
      END

      SUBROUTINE FILLRHS(NT,M,NRTD,C,RHS,JT,T)
C
C     Routine for filling in the RHS of the set of linear equations to be
C     solve.
C
      IMPLICIT REAL*8 (A-H,O-Z)
      DIMENSION C(NT), RHS(M), JT(NRTD), T(NRTD)
C
      DO 500 I=2,NT-3
         RHS(I)=C(I)
500   CONTINUE
      RHS(1)=C(1)-T(1)
      RHS(NT-2)=C(NT-2)-T(NRTD)

      DO 510 I=2,NRTD-1
         RHS(NT+JT(I)-3)=2.*T(I)
510   CONTINUE
      RETURN
      END

      SUBROUTINE FITPROF(T,XT,M,THETA,NT,DX)
      IMPLICIT REAL*8 (A-H,O-Z)
      DIMENSION T(M),XT(M)
      DIMENSION THETA(NT)
      DIMENSION X(3,3), XAUX(3,3), R(3), RAUX(3)

C
C
C-----FIT PARABOLA
C
      IF(M .EQ. 3) THEN
        DO 520 I=1,3
          X(I,1)=XT(I)*XT(I)
          X(I,2)=XT(I)
          X(I,3)=1.
          R(I)=T(I)
520     CONTINUE
      ELSE
        DO 530 I=1,M
          XSUM=XSUM+XT(I)
          X2SUM=X2SUM+XT(I)*XT(I)
          X3SUM=X3SUM+XT(I)*XT(I)*XT(I)
          X4SUM=X4SUM+XT(I)*XT(I)*XT(I)*XT(I)
          XTSUM=XTSUM+XT(I)*T(I)
          X2TSUM=X2TSUM+XT(I)*XT(I)*T(I)
          TSUM=TSUM+T(I)
530     CONTINUE
        X(1,1)=X4SUM
        X(1,2)=X3SUM
        X(1,3)=X2SUM
        X(2,1)=X3SUM
        X(2,2)=X2SUM
        X(2,3)=XSUM
```

```
        X(3,1)=X2SUM
        X(3,2)=XSUM
        X(3,3)=M
        R(1)=X2TSUM
        R(2)=XTSUM
        R(3)=TSUM
      ENDIF

      CALL MATSOL(3,3,X,R,XAUX,RAUX,1)
      DO 540 I=1,NT
        XX=(I-1)*DX
        THETA(I)=R(1)*XX*XX+R(2)*XX+R(3)
540   CONTINUE
C
      RETURN
      END

      SUBROUTINE MATSOL(M,MMAX,A,B,AA,BB,IOPT)
      IMPLICIT REAL*8 (A-H,O-Z)
      DIMENSION A(MMAX,MMAX), B(M)
      DIMENSION AA(MMAX,MMAX), BB(M)
      DO 500 I=1,M
        BB(I)=B(I)
        DO 510 J=1,M
          AA(I,J)=A(I,J)
510     CONTINUE
500   CONTINUE
C      WRITE(*,*)
C      DO 520 I=1,M
C        WRITE(*,'(1X,<M>F6.2,3X,F6.2)') (A(I,J),J=1,M),B(I)
C520   CONTINUE

      DO 530 K=2,M
        IF(IOPT .NE. 0) THEN
C
C-------FIND OPTIMUM 'TOP' ROW
C
C         PRINT*,'A:'
C         DO 540 I=1,M
C           WRITE(*,'(10F8.3)') (A(I,J),J=1,M),B(I)
C540      CONTINUE
          K1=K-1
          AMAX=ABS(A(K-1,K-1))
          DO 550 KK=K,M
            IF(ABS(A(KK,K-1)) .GT. AMAX) THEN
              K1=KK
              AMAX=ABS(A(KK,K-1))
            ENDIF
550       CONTINUE
          IF(K1.NE.K-1) THEN
            DO 560 I=K-1,M
              ADUM=A(K-1,I)
              A(K-1,I)=A(K1,I)
              A(K1,I)=ADUM
560         CONTINUE
            BDUM=B(K-1)
            B(K-1)=B(K1)
            B(K1)=BDUM
          ENDIF
        ENDIF
C         PRINT*,'B:'
C         DO 570 I=1,M
C           WRITE(*,'(10F8.3)') (A(I,J),J=1,M),B(I)
C570      CONTINUE
C
C---------------
C
          DO 580 I=K,M
            B(I)=B(I)-B(K-1)*(A(I,K-1)/A(K-1,K-1))
            DO 590 J=K,M
              A(I,J)=A(I,J)-A(I,K-1)*(A(K-1,J)/A(K-1,K-1))
590         CONTINUE
580       CONTINUE
C         PRINT*,'C:'
C         DO 600 I=1,M
C           WRITE(*,'(1X,<M>F6.2,3X,F6.2)') (A(I,J),J=1,M),B(I)
C600      CONTINUE
530     CONTINUE


        B(M)=B(M)/A(M,M)
        DO 610 I=M-1,1,-1
          DO 620 J=I+1,M
            B(I)=B(I)-A(I,J)*B(J)
```

```
620     CONTINUE
        B(I)=B(I)/A(I,I)
610   CONTINUE
C
C       DO 630 I=1,M
C         WRITE(*,*) (A(I,J),J=1,M),B(I)
C630    CONTINUE
C
      RMAX=0.
      DO 640 I=1,M
        S=0.
        DO 650 J=1,M
          S=S+AA(I,J)*B(J)
650     CONTINUE
        R=ABS(S-BB(I))
        IF(ABS(R) .GT. RMAX) RMAX=R
C        WRITE(*,'(1X,G12.5,10X,G12.5)') B(I), R

640   CONTINUE
      IF(RMAX .GT. 1.E-10)
     +  WRITE(*,'(A)') '*** WARNING, EQUATION SOLVER MAY BE',
     +                 ' INACCURATE ***'

      RETURN
      END
```

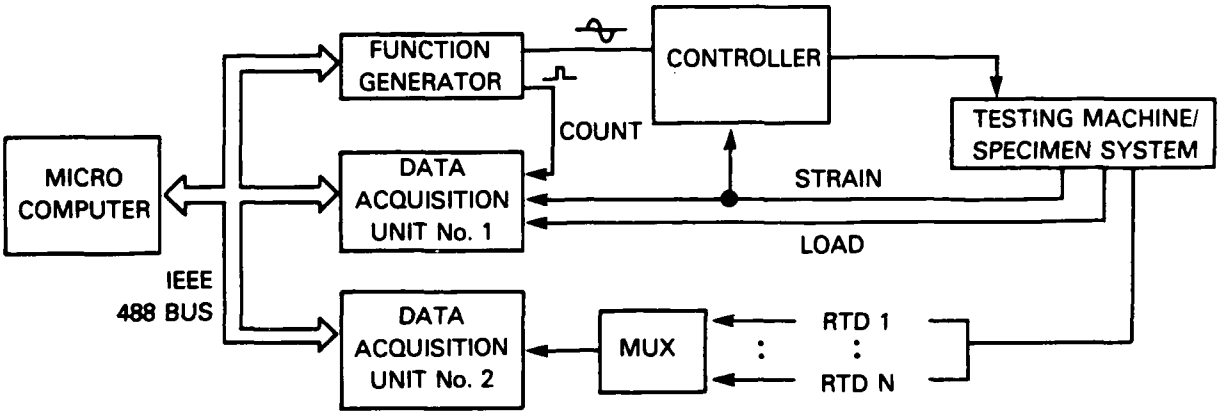

Figure 1 — Experimental Set-up

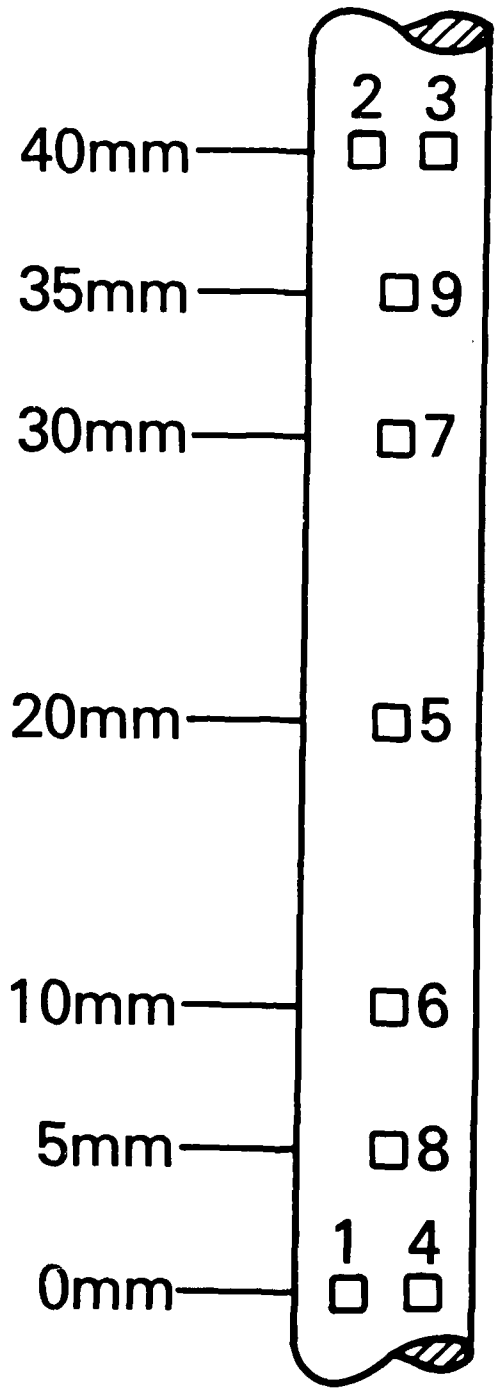

Figure 2a — RTD Locations for Testing Frequency of 1 Hz

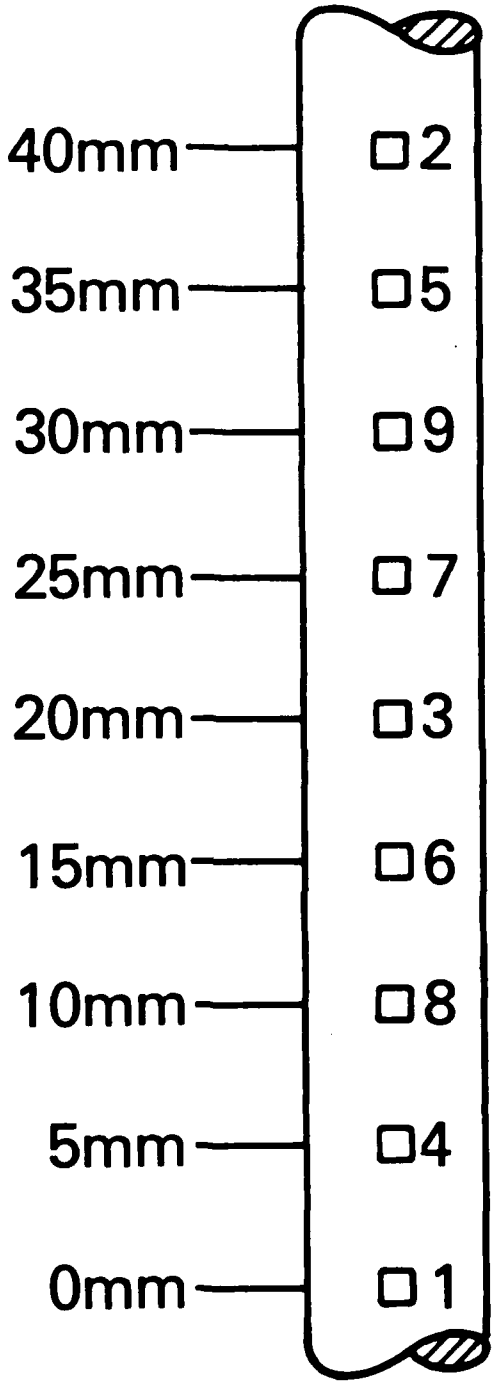

Figure 2b — RTD Locations for Testing Frequency of 4 Hz

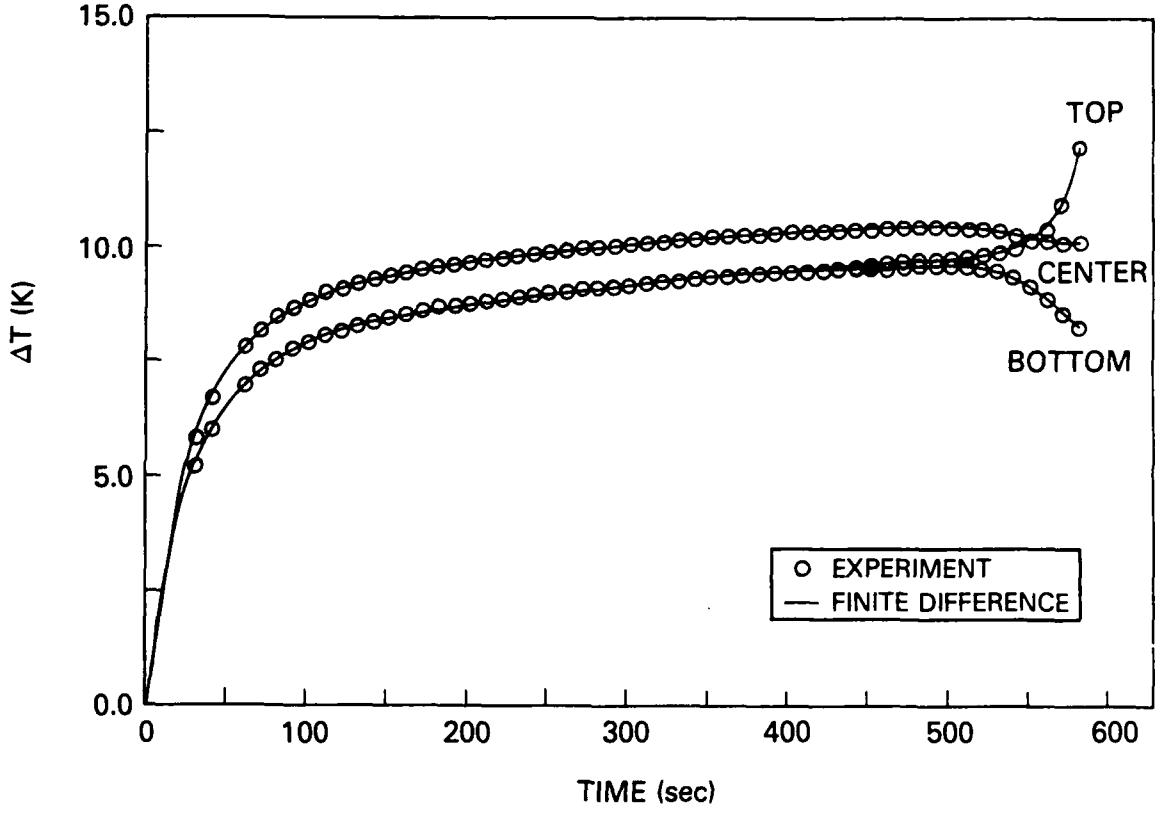

Figure 3 — Temperature History, 1 Hz, $\epsilon = \pm 0.52\%$

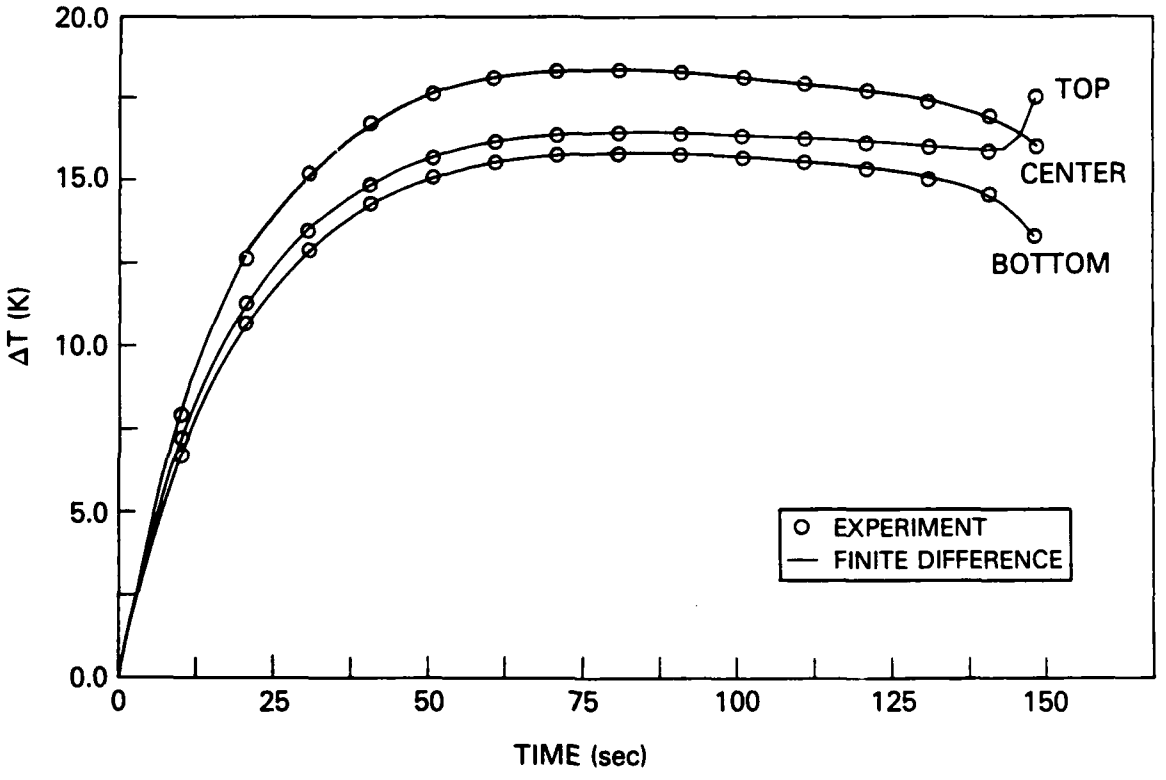

Figure 4 — Temperature History, 4 Hz, $\epsilon = \pm 0.45\%$

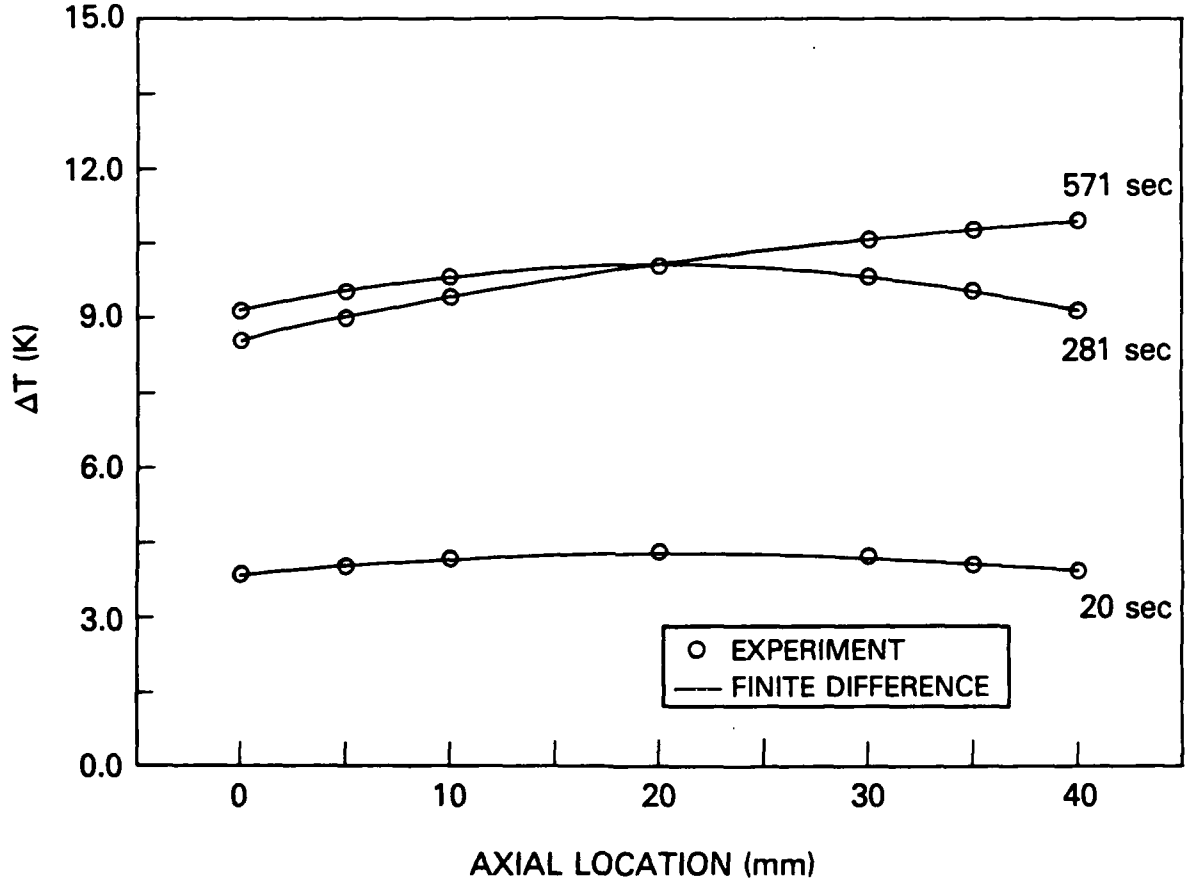

Figure 5 — Temperature Profile 1 Hz, $\epsilon = \pm 0.52\%$

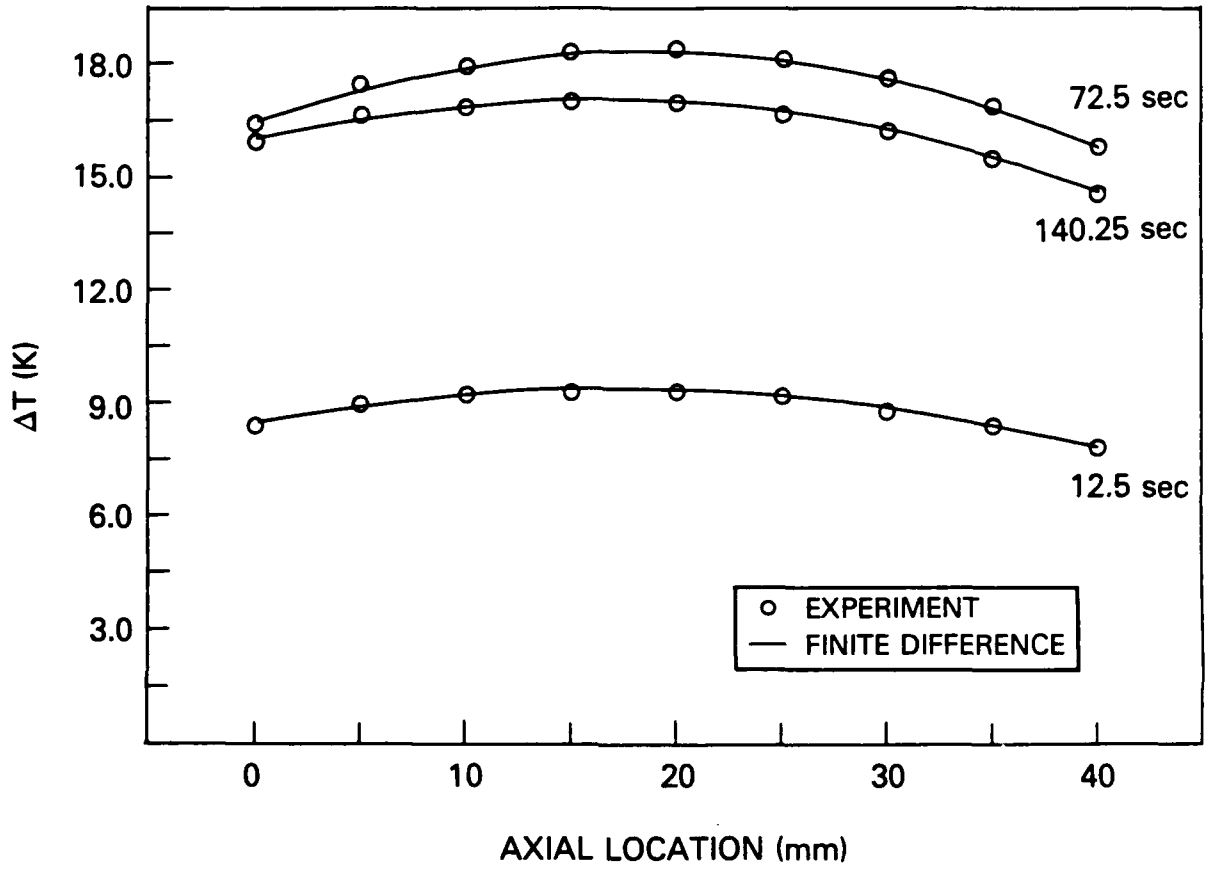

Figure 6 — Temperature Profile 4 Hz, $\epsilon = \pm 0.45\%$

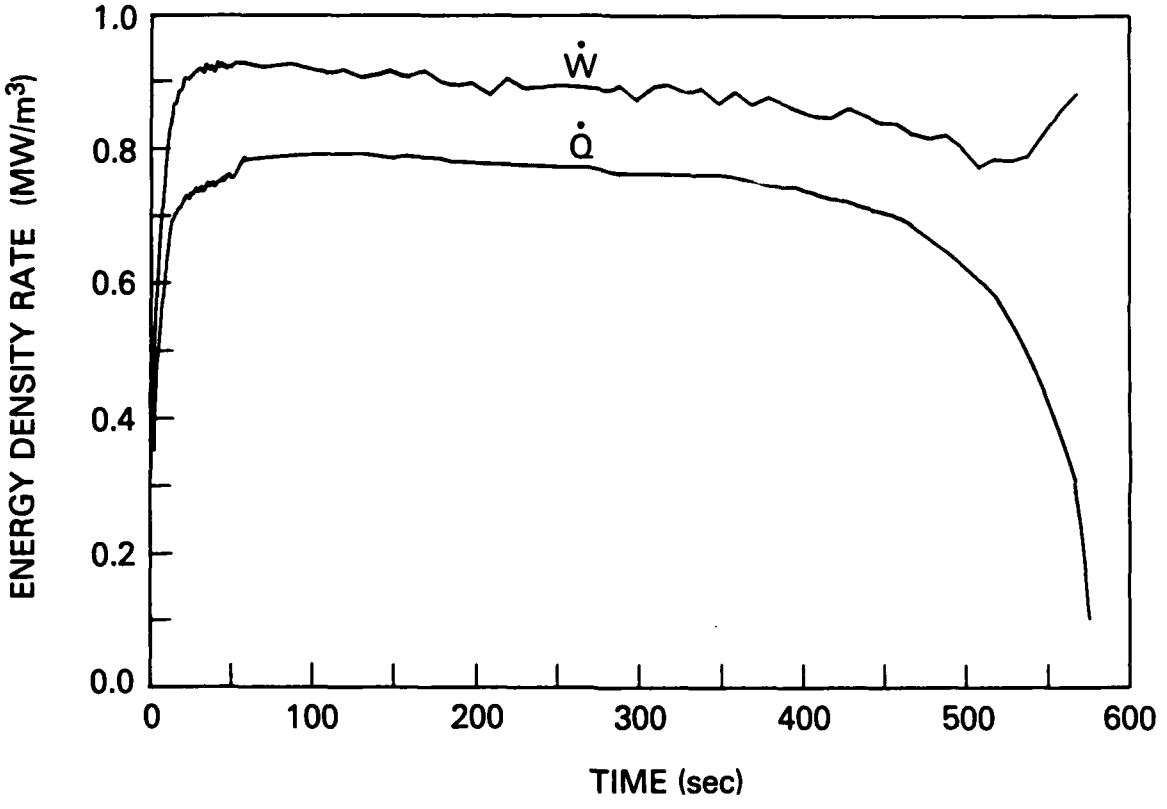

Figure 7 — Energy Density Rate History 1 Hz, $\epsilon = \pm 0.52\%$

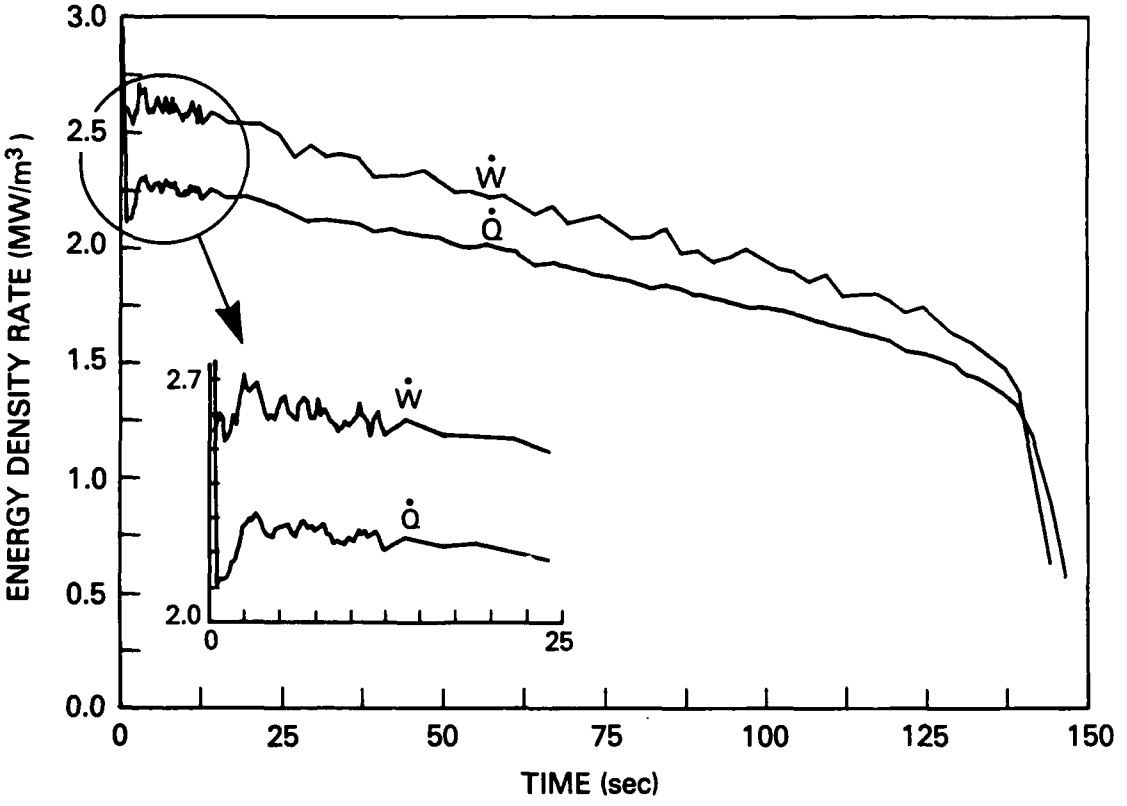

Figure 8 — Energy Density Rate Histories, 4 Hz, $\epsilon = \pm 0.45\%$

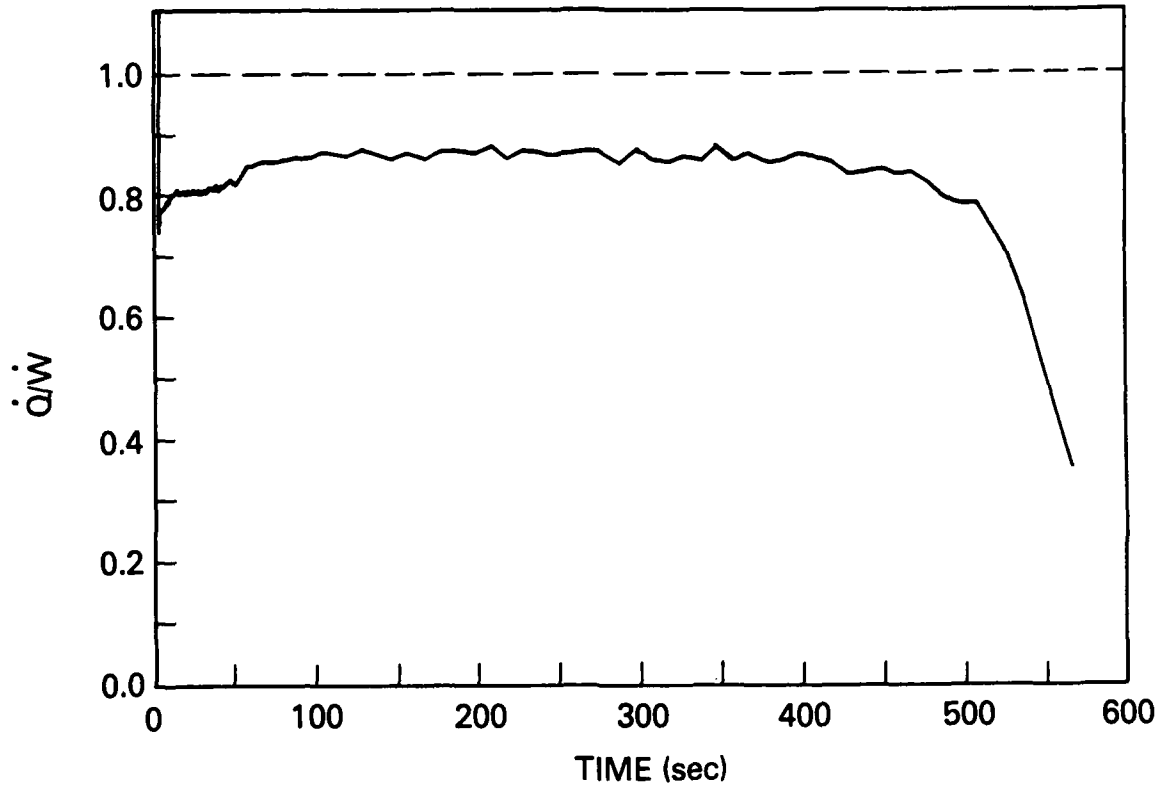

Figure 9 — Work-Heat Conversion Efficiency 1 Hz, $\epsilon = \pm 0.52\%$

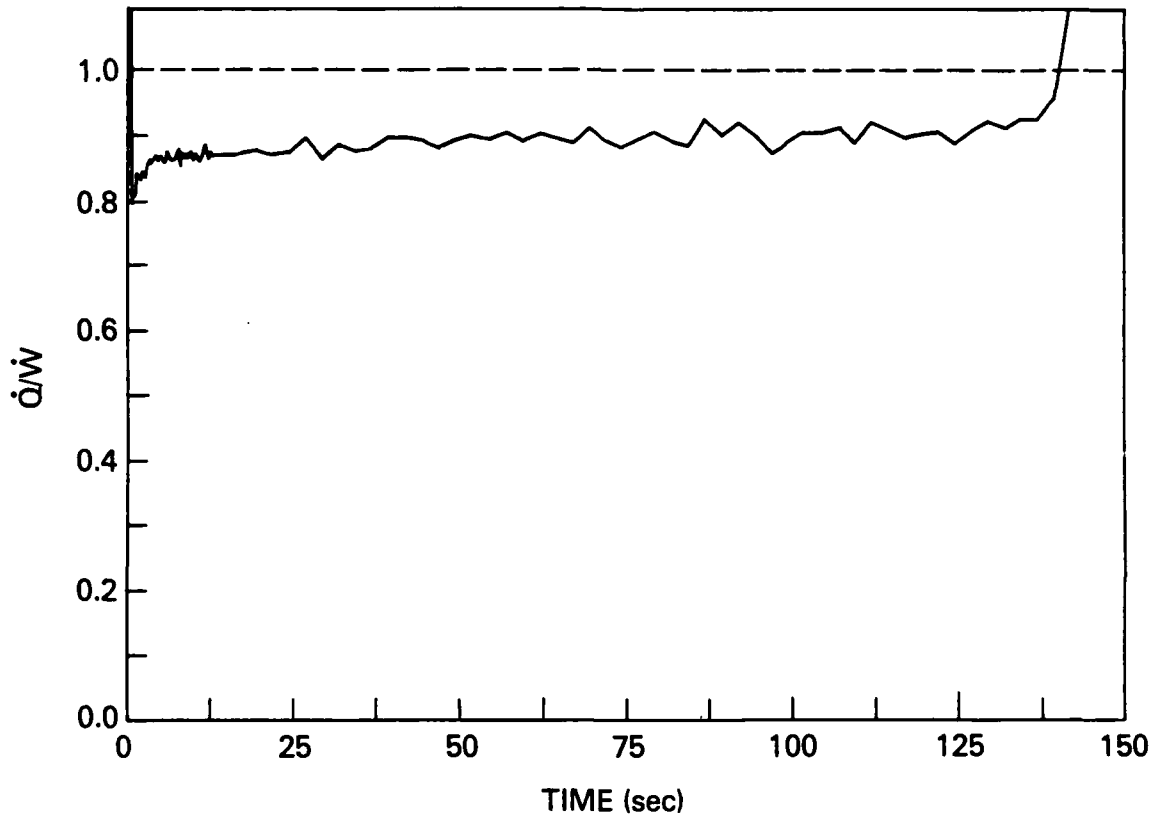

Figure 10 — Work-Heat Conversion Efficiency 4 Hz, $\epsilon = \pm 0.45\%$

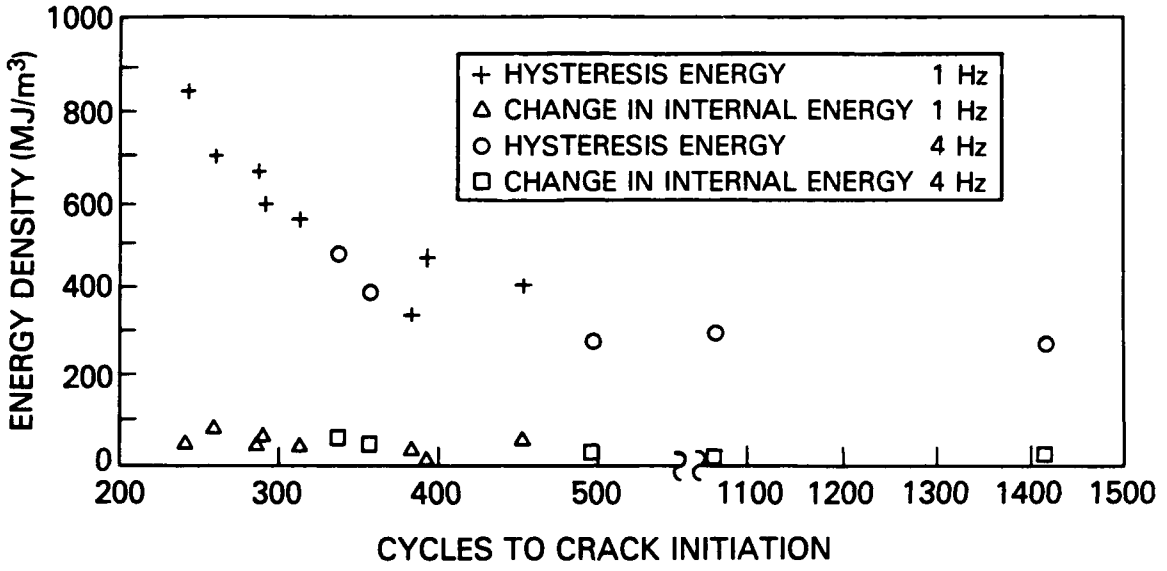

Figure 11 — Total Energy Densities to Crack Initiation